Available online at www.sciencedirect.com
ScienceDirect
International Journal of Heat and Mass Transfer 50 (2007) 1545–1558
International Journal of HEAT and MASS TRANSFER
www.elsevier.com/locate/ijhmt

Performance and optimization analysis of SRC profile fins subject to simultaneous heat and mass transfer

B. Kundu

Department of Mechanical Engineering, Jadavpur University, Kolkata 700 032, India

Received 23 March 2005; received in revised form 25 August 2006
Available online 2 November 2006

Abstract

Fin material near the tip of a uniform cross sectional (UC) fin does not participate actively in transferring heat. This effect may seem to have progressed much with the increase in fin length. A uniform cross sectional fin with a step reduction in local cross section (SRC) not only increases the effective utilization of fin material near the tip but also it promotes the ease of fabrication. In this study, an effort has been devoted to determine analytically the overall fin performance of both longitudinal and pin fins of SRC profile under fully dry, partially wet and fully wet conditions. The effect of various design and psychometric parameters on the fin performance of SRC fins has been investigated and compared it is with the corresponding UC fin. A scheme for optimizing SRC fins has also been demonstrated in the present work. From the result, it can be highlighted that the optimum values of Biot number and aspect ratio of SRC fins increase with the increase in relative humidity for the same fin volume. In comparison with the UC fin for the identical fin volume, the SRC fin transfers more rate of heat and consequently, this difference in heat transfer rate increases slowly with the relative humidity.

Keywords: Dehumidification; Longitudinal fin; Fin efficiency; Material saving; Optimization; Pin fin; SRC profile fin

1. Introduction

Technology has led to a demand for high performance, lightweight, and compact heat transfer equipments. To provide accommodation this demand, finned surfaces are usually used to increase the rate of heat transfer between a primary surface and the surrounding fluid in various heat exchangers. There are a plenty of practical applications of fins in heat transfer appliances, especially, the design of cooling devices for spacecrafts, and the evaporator of refrigeration and air conditioning equipments play the key role for successful applications. In these apparatus, the surface temperature of the fin is below the dew point temperature of the surrounding humid air. As a result, moisture is condensed on the fin surfaces and thus mass transfer occurs simultaneously with heat transfer. Depending upon the primary surface temperature, the fin tip temperature and the dew point of the surrounding air, the fin surface may be classified as full dry, partially wet or fully wet [1,2]. The thermal performance of the wet extended surface is different from that of the dry surface as the moisture condenses on the fin surfaces during dehumidification process.

Numerous investigations have been carried out by many researchers to determine the performance of fins under dehumidifying conditions. Threlkeld [1] adopted an analogous approach to establish the influence of water film on the performance of wet rectangular fins. From his observation, he demonstrated that the effect of relative humidity on the performance of wet fins is negligibly small. McQuiston [2] included the mass transfer phenomenon which is occurred due to difference in humidity ratio between the incoming air and that existed on the fin surface. His results indicate that the overall efficiency has been influenced strongly by the relative humidity. Assuming a linear relationship between the humidity ratio of the saturated air on the fin surface and its temperature, Elmahdy and Biggs [3] presented a numerical algorithm to evaluate the

E-mail address: bkundu123@rediffmail.com

0017-9310/$ - see front matter © 2006 Elsevier Ltd. All rights reserved.
doi:10.1016/j.ijheatmasstransfer.2006.08.029

Nomenclature

A, B	constants, expressed in Eq. (11)
Bi	Biot number, $h\delta_b/k$
$C_{p,a}$	specific heat of dry air at constant pressure
f_1, f_2, f_3	functions, used in Eq. (39)
g	function for the constraint, used in Eq. (40)
h	convective heat transfer coefficient, kJ/m^2 K
h_{fg}	latent heat of condensation of moisture, kJ/kg
h_m	mass transfer coefficient, kg/m^2 s
k	thermal conductivity of the fin material, W/m K
l	fin length, m
l_0	distance from the base at which the dry and wet region separated, m
l_S	distance from the base where step change is made, m
L_0	dimensionless linear distance at which dry and wet part coexisted, l_0/L
Le	Lewis number
L_S	dimensionless step length, l_S/l
m	constant 1 and 2 for longitudinal fin and pin fin, respectively
q	heat transfer rate, W
Q	dimensionless heat transfer rate, $qh^{m-1}m/[2k^m(T_a - T_b)\pi^{m-1}]$
Q_r	percentage increase in heat transfer rate of a step profile fin with respect to a rectangular profile fin
RH	relative humidity of surrounding air
SRC	step reduction in cross section
T	local fin surface temperature, °C
U	dimensionless fin volume, $h^{m+1}vm/[2k^{m+1}\pi^{m-1}]$
UC	uniform cross section
v	respectively fin volume per unit width for the longitudinal fin and fin volume for the pin fin, m^3
x	coordinate as shown in Fig. 1, m
X	dimensionless coordinate, x/l
Z_0	fin parameter, $\sqrt{Bi}/\psi$
Z_1	$Z_0/\sqrt{\mu}$
Z_2	$Z_0(1 + B\xi)^{1/2}$
Z_3	$Z_1(1 + B\xi)^{1/2}$

Greek symbols

δ	half fin thickness, m
ε	fin effectiveness
ϕ	temperature parameter, $\theta + \theta_w$
η	fin efficiency
μ	ratio of tip to base half-thickness, δ_t/δ_b
θ	dimensionless local fin surface temperature, $(T_a - T)/(T_a - T_b)$
θ_w	temperature parameter for dehumidification, $\xi(\omega_a - A - BT_a)/[(T_a - T_b)(1 + B\xi)]$
ω	specific humidity, kg w.v./kg d.a.
ξ	dimensionless dehumidification parameter, $h_{fg}/C_pLe^{2/3}$
ψ	aspect ratio, δ_b/L

Subscripts

a	ambient
b	base
d	dew point
dry	dry surface
id	ideal
p	partially wet
t	tip
wet	wet surface

efficiency of longitudinal and circular fins of uniform thickness when simultaneous heat and mass transfer take place. Their result shows that the fin efficiency does have a strong dependency on relative humidity.

Coney et al. [4,5] developed a model to study the influence of the condensate layer on the surface temperature distribution and efficiency of a wet rectangular fin. This model indicates that the fin efficiency decreases with the condensation. Kazeminejad et al. [6] demonstrated the effect of relative humidity on the thermal resistance of condensate film and it was negligible as the film found to be much thinner than the boundary layer in the dehumidification process. Their model exhibits that the heat transfer coefficient is changed with the increase in boundary layer thickness. Wu and Bong [7] provided an analytical solution to determine the overall fin performance of a rectangular fin under both fully and partially wet conditions. They also assumed a negligible film thickness and, temperature and humidity ratio difference as the driving force for heat and mass transfer. Lin et al. [8] studied experimentally the performance of a rectangular fin in both dry and wet conditions. They found that the fully wet fin efficiency was insensitive to change of relative humidity. For comparison purposes, the fin efficiency of their experimental data agrees favorably with the predictive analytical results obtained by Wu and Bong [7].

The above studies were based on the one-dimensional approach. For detailed evaluation of the wet fin efficiency, Chen [9] and Liang et al. [10] proposed a two-dimensional model that took the complex fin and the moist air properties over the fin into account. These two investigations supported that the fully wet fin efficiency was moderately insensitive to change of relative humidity.

In search of a reduction of material of a fin, a comprehensive research has already been exhibited to determine an optimum profile of fins under convective environment. A criterion for obtaining the optimum profile of conducting-convective fins was first proposed heuristically

by Schmidt [11]. Later, Duffin [12] had proved mathematically the Schmidt [11] criterion by using the calculus of variation. From the existing literature [13–15], it can be found that the optimum profiles are parabolic, hyperbolic, circular or wavy in nature. Fabbri [16] has introduced undulations in the optimum fin profile by using genetic algorithms. However, these profiles are associated with inherent difficulties for their manufacturing and fabrication. Hence, an alternative approach is generally adopted by the researchers for the optimum design of a fin [17,18]. In this methodology, a fin shape is selected a priory and then the optimum dimensions are determined with satisfying either maximizing the heat transfer rate for a given fin volume or minimizing the fin volume for a given heat transfer duty.

A quasilinear one-dimensional model was developed by Kilic and Onat [19] to calculate the fin performance and optimum dimensions of a vertical rectangular wet fin. They investigated that the optimum fin length, fin effectiveness and average fin temperature are lower in the case of condensation than in the case of dry fin. Toner et al. [20] numerically established a comparison between the rectangular and triangular fins when condensation takes place. They also calculated the optimum fin dimensions. Using Bessel functions, Kundu [21] determined analytically the optimum dimensions of fully wet straight tapered fins. Recently, by application through a unified analysis, an analytical model has been suggested by Kundu and Das [22] for the estimation of optimum fin dimensions of fully wet longitudinal, spine and annular fins of both trapezoidal and triangular profiles.

Even though a tapered profile fin reduces the fin material, it is not applied to all heat exchange applications, probably, owing to its typical geometry. Otherwise, due to simple design and ease of fabrications, the uniform cross sectional (UC) fin is extensively found in various heat exchangers. However, there is a continuous effort to modify this shape near the tip for betterment of its performance. Holland and Stedman [23] proposed first to modify for a constant thickness fin known as rectangular fin with a step change in local thickness. A reduction in plate material can be achieved with the applying this profile. However, their analysis had been concentrated only on the absorber plate of a flat plate collector. Later Kundu and Das [24] have extended this approach to analyze the performance and optimization of annular step fins subject to convective environment. They have mentioned that an annular step rectangular fin saves 30% or more material in comparison to an annular rectangular fin for the same heat transfer duty.

So far, there have been many investigations (summarized above) of different profiles, namely, rectangular, trapezoidal and triangular dealing with the wet surface subject to simultaneous heat and mass transfer applications. A significant material saving has already been noticed by using a stepped annular fin under the dry surface condition [24]. However, researchers have rarely concentrated on the thermal analysis of both longitudinal and pin fins with a step reduction in cross section (SRC) under the process of dehumidification. In addition, a few of the literatures are concerned with pin fins, in spite of the fact that pin fins are frequently employed in lot of real applications.

In the present study, an effort has been made to analyze analytically the performance and optimization of longitudinal and pin fins of SRC profile subject to combined heat and mass transfer. The analysis is carried out for the fully dry, partially wet and fully wet conditions on fin surfaces. The present analysis is also suitable for the UC fin with choosing the unit value of thickness ratio of a SRC fin. A comparative study on fin performances between SRC and UC fins has also been done for the same thermophysical and psychometric conditions. In addition, a methodology has been suggested for the optimization of SRC fins in wet conditions. The optimization has been cast in a generalized form such that either fin volume or heat transfer duty can be taken as a constraint. Using Lagrange multiplier techniques, the optimality criteria are derived. A generalized Newton–Raphson iterative method is used to determine the optimum design parameters. A comparative study between SRC and UC fins at the optimum condition has also been made. Finally, it may be well established that within the range of design parameters taken in the present analysis, the amount of heat transfer rate through an optimum fin of SRC is 20% or more than that of an optimum UC fin with an identical fin volume and psychometric properties of surrounding air.

2. Physical model and mathematical formulations

The physical model of longitudinal and pin fins with SRC profile is depicted in Fig. 1, where l is the fin height, l_S is the distance from the base at which step change occurs, δ_b and δ_t are the half fin thicknesses of the base and tip side respectively. When humid air strikes on a fin surface below its dew point temperature, T_d, the moisture condenses on its in filmwise, dropwise or mixed mode, depending upon the condition of the wet surface. In general, a clean surface tends to promote filmwise condensation whereas a treated surface condensates dropwise. If the condensation takes place continuously over the fin surface and the condensed liquid is removed from the surface by the motion generated from gravity, then the condensing surface is usually covered with a thin layer of liquid; and this situation is known as film wise condensation. The presence of condensate on the cooling surface may enhance heat and mass transfer at the surface due to increased turbulence and effective surface roughness. However, due to the build-up of much thinner condensate film with the boundary layer in the dehumidification process, the effect of condensate film has been omitted by many investigators [6–8,20–22]. The difference between air and fin surface temperatures is the driving force for sensible heat transfer and accordingly, the difference between humidity ratio of surrounding air and that of the adjacent air on the fin surface is the driving

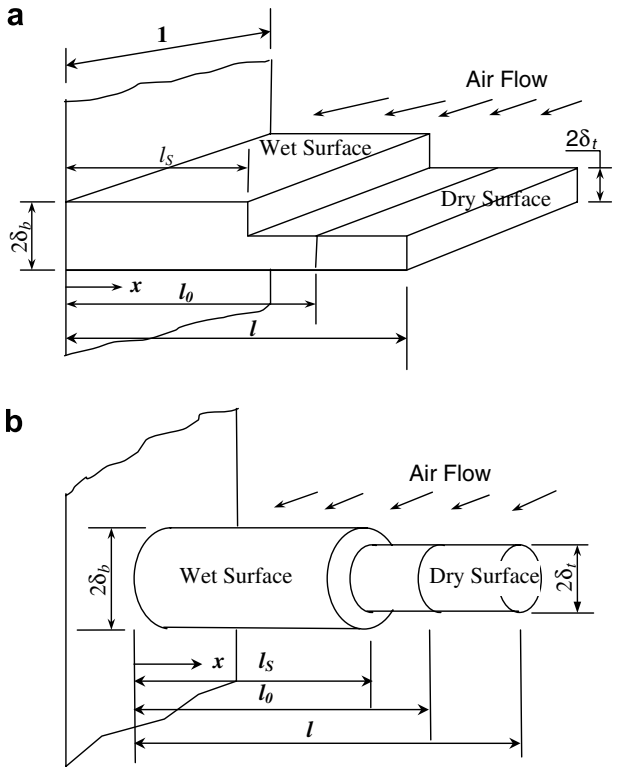

Fig. 1. Schematic view of partially wet SRC fins with a length parameter L_0 at which dry and wet surfaces separated: (a) longitudinal fin and (b) pin fin.

force for mass transfer. To establish the present theoretical model, the following assumptions are made:

(i) The fin base temperature, T_b, and the dry bulb temperature of the surrounding air, T_a, are assumed to be constant.
(ii) Due to the 'thin fin' assumption, the temperature variation on the fin surface in the perpendicular direction is negligibly small and temperature varies only in the x direction.
(iii) The convective heat transfer coefficient (h) is assumed to be constant for all over the fin surfaces.
(iv) The thermal conductivity of the fin material (k) is taken constant.
(v) Thermal resistance for heat flow through condensate film is negligibly small.
(vi) Specific humidity ω on the fin surface air can be approximated by a straight line ($\omega = A + BT$) with the saturated water film temperature T, for having a small temperature difference between dew point and fin-base temperature.

2.1. Governing equations

To establish the governing equations for both the stepped longitudinal and pin fins, fin surfaces are considered a fully dry, fully wet or partially wet. The governing differential equations derived from an energy balance on a differential volume element of a SRC fin under steady state condition can be written as follows:

Fully dry fin

$$\begin{bmatrix} d^2T/dx^2 - mh(T-T_a)/k\delta_b \\ d^2T/dx^2 - mh(T-T_a)/k\delta_t \end{bmatrix} = \begin{bmatrix} 0 \\ 0 \end{bmatrix} \quad \begin{matrix} \text{for } (0 \leqslant x \leqslant l_S) \\ \text{for } (l_S \leqslant x \leqslant l) \end{matrix} \tag{1}$$

Fully wet fin

$$\begin{bmatrix} d^2T/dx^2 - mh(T-T_a)/k\delta_b - mh_m(\omega-\omega_a)h_{fg}/k\delta_b \\ d^2T/dx^2 - mh(T-T_a)/k\delta_t - mh_m(\omega-\omega_a)h_{fg}/k\delta_t \end{bmatrix} = \begin{bmatrix} 0 \\ 0 \end{bmatrix} \quad \begin{matrix} \text{for } (0 \leqslant x \leqslant l_S) \\ \text{for } (l_S \leqslant x \leqslant l) \end{matrix} \tag{2}$$

Partially wet fin ($l_S \leqslant l_0 < l$)

$$\begin{bmatrix} d^2T/dx^2 - mh(T-T_a)/k\delta_b - mh_m(\omega-\omega_a)h_{fg}/k\delta_b \\ d^2T/dx^2 - mh(T-T_a)/k\delta_t - mh_m(\omega-\omega_a)h_{fg}/k\delta_t \\ d^2T/dx^2 - mh(T-T_a)/k\delta_t \end{bmatrix} = \begin{bmatrix} 0 \\ 0 \\ 0 \end{bmatrix} \quad \begin{matrix} \text{wet domain } (0 \leqslant x \leqslant l_S) \\ \text{wet domain } (l_S \leqslant x \leqslant l_0) \\ \text{dry domain } (l_0 \leqslant x \leqslant l) \end{matrix} \tag{3}$$

Partially wet fin ($0 < l_0 \leqslant l_S$)

$$\begin{bmatrix} d^2T/dx^2 - mh(T-T_a)/k\delta_b - mh_m(\omega-\omega_a)h_{fg}/k\delta_b \\ d^2T/dx^2 - mh(T-T_a)/k\delta_b \\ d^2T/dx^2 - mh(T-T_a)/k\delta_t \end{bmatrix} = \begin{bmatrix} 0 \\ 0 \\ 0 \end{bmatrix} \quad \begin{matrix} \text{wet domain } (0 \leqslant x \leqslant l_0) \\ \text{dry domain } (l_0 \leqslant x \leqslant l_S) \\ \text{dry domain } (l_S \leqslant x \leqslant l) \end{matrix} \tag{4}$$

where h_m is the average mass transfer coefficient, ω_a is the humidity ratio of the atmospheric air, and h_{fg} is the latent heat of condensation. The constant m used in Eqs. (1)–(4) is 1 and 2 for the longitudinal and the pin fin, respectively.

The following dimensionless parameters can be introduced for the mathematical formulation:

$$X = x/l, \quad L_0 = l_0/l, \quad L_S = l_S/l, \quad \psi = \delta_b/l,$$
$$Bi = h\delta_b/k, \quad \mu = \delta_t/\delta_b, \quad Z_0 = \sqrt{Bi}/\psi,$$
$$Z_1 = Z_0/\sqrt{\mu} \quad \text{and} \quad \theta = (T_a - T)/(T_a - T_b) \tag{5}$$

The heat transfer and mass transfer coefficient can be related by Chilton–Colburn analogy [25] given by

$$h/h_m = C_{p,a}Le^{2/3} \tag{6}$$

where Le and $C_{p,a}$ are the Lewis number and specific heat of dry air, repectively.

Using Chilton–Colburn analogy [25] and the above assumptions, Eqs. (1)–(4) can be expressed in dimensionless form respectively as

Fully dry fin

$$\begin{bmatrix} \mathrm{d}^2\theta/\mathrm{d}X^2 - mZ_0^2\theta \\ \mathrm{d}^2\theta/\mathrm{d}X^2 - mZ_1^2\theta \end{bmatrix} = \begin{bmatrix} 0 \\ 0 \end{bmatrix} \quad \begin{matrix} (0 \leqslant X \leqslant L_S) \\ (L_S \leqslant X \leqslant 1) \end{matrix} \tag{7}$$

Fully wet fin

$$\begin{bmatrix} \mathrm{d}^2\phi/\mathrm{d}X^2 - mZ_0^2(1+B\xi)\phi \\ \mathrm{d}^2\phi/\mathrm{d}X^2 - mZ_1^2(1+B\xi)\phi \end{bmatrix} = \begin{bmatrix} 0 \\ 0 \end{bmatrix} \quad \begin{matrix} (0 \leqslant X \leqslant L_S) \\ (L_S \leqslant X \leqslant 1) \end{matrix} \tag{8}$$

Partially wet fin ($L_S \leqslant L_0 < 1$)

$$\begin{bmatrix} \mathrm{d}^2\phi/\mathrm{d}X^2 - mZ_0^2(1+B\xi)\phi \\ \mathrm{d}^2\phi/\mathrm{d}X^2 - mZ_1^2(1+B\xi)\phi \\ \mathrm{d}^2\theta/\mathrm{d}X^2 - mZ_1^2\theta \end{bmatrix} = \begin{bmatrix} 0 \\ 0 \\ 0 \end{bmatrix} \quad \begin{matrix} \text{wet domain } (0 \leqslant X \leqslant L_S) \\ \text{wet domain } (L_S \leqslant X \leqslant L_0) \\ \text{dry domain } (L_0 \leqslant X \leqslant 1) \end{matrix} \tag{9}$$

Partially wet fin ($0 < L_0 \leqslant L_S$)

$$\begin{bmatrix} \mathrm{d}^2\phi/\mathrm{d}X^2 - mZ_0^2(1+B\xi)\phi \\ \mathrm{d}^2\theta/\mathrm{d}X^2 - mZ_0^2\theta \\ \mathrm{d}^2\theta/\mathrm{d}X^2 - mZ_1^2\theta \end{bmatrix} = \begin{bmatrix} 0 \\ 0 \\ 0 \end{bmatrix} \quad \begin{matrix} \text{wet domain } (0 \leqslant X \leqslant L_0) \\ \text{dry domain } (L_0 \leqslant X \leqslant L_S) \\ \text{dry domain } (L_S \leqslant X \leqslant 1) \end{matrix} \tag{10}$$

where

$$\begin{aligned} &\phi = \theta + \theta_w, \quad \xi = h_{fg}/(C_{p,a}Le^{2/3}), \\ &\theta_w = \xi(\omega_a - A - BT_a)/[(T_a - T_b)(1+B\xi)], \\ &A = [\omega_b(T_t - T_a) - T_b(\omega_t - \omega_b)]/(T_t - T_b) \quad \text{and} \\ &B = (\omega_t - \omega_b)/(T_t - T_b) \end{aligned} \tag{11}$$

2.2. Boundary conditions

Since the fin base temperature is lower than that of the fin tip, heat conduction through a fin takes place from the fin tip to fin base. Depending upon the fin surface temperature and dew point temperature of the surrounding air, energy interaction between the surrounding air and the fin surface occurs on all over the exposed surfaces with either sensible heat or both sensible and latent heat. An energy balance can be done at the junction section L_S to satisfy the continuity of heat conduction and the heat exchange between the excess fin thickness surface and the surrounding medium. In case of partially wet fins, there is a position on the fin surface L_0 (shown in Fig. 1), where the surface temperature is equal to the dew point of the humid air. Hence, $X = L_0$ separates the dry and wet regions. Thus, the boundary conditions to determine temperature distribution in SRC fins are taken mathematically as follows:

Fully dry fin

$$\text{at } X = 0, \quad \theta = 1 \tag{12a}$$

$$\text{at } X = L_S, \quad \begin{cases} [\theta]_{L_S-\Delta} = [\theta]_{L_S+\Delta} \\ [\mathrm{d}\theta/\mathrm{d}X]_{L_S-\Delta} = \mu^m[\mathrm{d}\theta/\mathrm{d}X]_{L_S+\Delta} \\ \qquad -\psi Z_0^2(1-\mu^m)[\theta]_{L_S-\Delta} \end{cases} \tag{12b}$$

$$\text{at } X = 1, \quad \mathrm{d}\theta/\mathrm{d}X = -\psi Z_0^2\theta \tag{12c}$$

Fully wet fin

$$\text{at } X = 0, \quad \phi = 1 + \theta_w \tag{13a}$$

$$\text{at } X = L_S, \quad \begin{cases} [\phi]_{L_S-\Delta} = [\phi]_{L_S+\Delta} \\ [\mathrm{d}\phi/\mathrm{d}X]_{L_S-\Delta} = \mu^m[\mathrm{d}\phi/\mathrm{d}X]_{L_S+\Delta} \\ \qquad -\psi Z_0^2(1-\mu^m)(1+B\xi)[\phi]_{L_S-\Delta} \end{cases} \tag{13b}$$

$$\text{at } X = 1, \quad \mathrm{d}\phi/\mathrm{d}X = -\psi Z_0^2(1+B\xi)\phi \tag{13c}$$

Partially wet fin ($L_S \leqslant L_0 < 1$)

$$\text{at } X = 0, \quad \phi = 1 + \theta_w \tag{14a}$$

$$\text{at } X = L_S, \quad \begin{cases} [\phi]_{L_S-\Delta} = [\phi]_{L_S+\Delta} \\ [\mathrm{d}\phi/\mathrm{d}X]_{L_S-\Delta} = \mu^m[\mathrm{d}\phi/\mathrm{d}X]_{L_S+\Delta} \\ \qquad -\psi Z_0^2(1-\mu^m)(1+B\xi)[\phi]_{L_S-\Delta} \end{cases} \tag{14b}$$

$$\text{at } X = L_0, \quad \begin{cases} \phi = \theta_d + \theta_w \\ \theta = \theta_d \end{cases} \tag{14c}$$

$$\text{at } X = 1, \quad \mathrm{d}\theta/\mathrm{d}X = -\psi Z_0^2\theta \tag{14d}$$

Partially wet fin ($0 < L_0 \leqslant L_S$)

$$\text{at } X = 0, \quad \phi = 1 + \theta_w \tag{15a}$$

$$\text{at } X = L_0, \quad \begin{cases} \phi = \theta_d + \theta_w \\ \theta = \theta_d \end{cases} \tag{15b}$$

$$\text{at } X = L_S, \quad \begin{cases} [\theta]_{L_S-\Delta} = [\theta]_{L_S+\Delta} \\ [\mathrm{d}\theta/\mathrm{d}X]_{L_S-\Delta} = \mu^m[\mathrm{d}\theta/\mathrm{d}X]_{L_S+\Delta} \\ \qquad -\psi Z_0^2(1-\mu^m)[\theta]_{L_S-\Delta} \end{cases} \tag{15c}$$

$$\text{at } X = 1, \quad \mathrm{d}\theta/\mathrm{d}X = -\psi Z_0^2\theta \tag{15d}$$

where $\Delta \to 0$.

2.3. Temperature profile

The temperature distribution in SRC fins is obtained by solving the above differential equations (7)–(10) with their boundary conditions (Eqs. (12) to (15)). Accordingly

Fully dry fin

$$\theta = \begin{cases} \dfrac{\sigma_1 \sinh[Z_1(1-L_S)] + \sigma_2 \cosh[Z_1(1-L_S)]}{\sigma_3 \sinh[Z_1(1-L_S)] + \sigma_4 \cosh[Z_1(1-L_S)]} \\ \quad \text{for } (0 \leqslant X \leqslant L_S) \\ \dfrac{Z_0\{Z_1 \cosh[Z_1(1-X)] + \psi Z_0^2 \sinh[Z_1(1-X)]\}}{\sigma_3 \sinh[Z_1(1-L_S)] + \sigma_4 \cosh[Z_1(1-L_S)]} \\ \quad \text{for } (L_S \leqslant X \leqslant 1) \end{cases} \tag{16}$$

where

$$\begin{bmatrix}\sigma_1\\ \sigma_2\\ \sigma_3\\ \sigma_4\end{bmatrix}=\begin{bmatrix}\psi Z_0^3\cosh[Z_0(L_S-X)]+Z_0^2\{1+(1-\mu^m)Z_0^2\psi^2\}\sinh[Z_0(L_S-X)]\\ Z_0Z_1\{\cosh[Z_0(L_S-X)]+\psi Z_0\sinh[Z_0(L_S-X)]\}\\ Z_0^2[\psi Z_0\cosh(Z_0L_S)+\{1+Z_0^2\psi^2(1-\mu^m)\}\sinh(Z_0L_S)]\\ Z_0Z_1[\cosh(Z_0L_S)+\psi Z_0\sinh(Z_0L_S)]\end{bmatrix} \tag{17}$$

Fully wet fin

$$\frac{\theta+\theta_w}{1+\theta_w}=\begin{cases}\dfrac{\sigma_5\sinh[Z_3(1-L_S)]+\sigma_6\cosh[Z_3(1-L_S)]}{\sigma_7\sinh[Z_3(1-L_S)]+\sigma_8\cosh[Z_3(1-L_S)]}\\ \quad\text{for } (0\leqslant X\leqslant L_S)\\ \dfrac{Z_2\{Z_3\cosh[Z_3(1-X)]+\psi Z_2^2\sinh[Z_3(1-X)]\}}{\sigma_7\sinh[Z_3(1-L_S)]+\sigma_8\cosh[Z_3(1-L_S)]}\\ \quad\text{for } (L_S\leqslant X\leqslant 1)\end{cases} \tag{18}$$

where

$$\begin{bmatrix}\sigma_5\\ \sigma_6\\ \sigma_7\\ \sigma_8\end{bmatrix}=\begin{bmatrix}\psi Z_2^3\cosh[Z_2(L_S-X)]+Z_2^2\{1+\psi^2Z_0^2(1-\mu^m)(1+B\xi)^{1/2}\}\sinh[Z_2(L_S-X)]\\ Z_2Z_3\{\cosh[Z_2(L_S-X)]+\psi Z_2\sinh[Z_2(L_S-X)]\}\\ Z_2^2\{\psi Z_2\cosh(Z_2L_S)+[1+\psi^2Z_0Z_2(1-\mu^m)]\sinh(Z_2L_S)\}\\ Z_2Z_3[\cosh(Z_2L_S)+\psi Z_2\sinh(Z_2L_S)]\end{bmatrix} \tag{19}$$

and

$$\begin{bmatrix}Z_2\\ Z_3\end{bmatrix}=\begin{bmatrix}Z_0(1+B\xi)^{1/2}\\ Z_1(1+B\xi)^{1/2}\end{bmatrix} \tag{20}$$

Partially wet fin ($L_S\leqslant L_0<1$)

$$\begin{bmatrix}\theta+\theta_w\\ \theta+\theta_w\\ \theta/\theta_d\end{bmatrix}=\begin{bmatrix}\dfrac{\sigma_{10}(1+\theta_w)\sinh[Z_2(L_S-X)]+\sigma_9\sinh(Z_2X)}{\sigma_{10}\sinh(Z_2L_S)}\\ \dfrac{\sigma_9\sinh[Z_3(L_0-X)]+\sigma_{10}(\theta_d+\theta_w)\sinh[Z_3(X-L_S)]}{\sigma_{10}\sinh[Z_3(L_0-L_S)]}\\ \dfrac{\psi Z_0^2\sinh[Z_1(1-X)]+Z_1\cosh[Z_1(1-X)]}{\psi Z_0^2\sinh[Z_1(1-L_0)]+Z_1\cosh[Z_1(1-L_0)]}\end{bmatrix}\begin{matrix}\text{for } (0\leqslant X\leqslant L_S)\\ \text{for } (L_S\leqslant X\leqslant L_0)\\ \text{for } (L_0\leqslant X\leqslant 1)\end{matrix} \tag{21}$$

where

$$\sigma_9=(1+\theta_d)Z_2\sinh[Z_3(L_0-L_S)]+(\theta_d+\theta_w)\mu^{m/2}Z_2\sinh(Z_2L_S) \tag{22}$$

and

$$\sigma_{10}=Z_2\cosh(Z_2L_S)\sinh(Z_4)+\mu^mZ_3\sinh(Z_2L_S)\times\cosh[Z_3(L_0-L_S)]+\psi Z_2^2(1-\mu^m)\sinh(Z_2L_S)\times\sinh[Z_3(L_0-L_S)] \tag{23}$$

Partially wet fin ($0<L_0\leqslant L_S$)

$$\begin{bmatrix}\theta+\theta_w\\ \theta\\ \theta\end{bmatrix}=\begin{bmatrix}\dfrac{(1+\theta_w)\sinh[Z_2(L_0-X)]+(\theta_d+\theta_w)\sinh(Z_2X)}{\sinh(Z_2L_0)}\\ \dfrac{\theta_d\sigma_{12}\sinh[Z_0(L_S-X)]+\sigma_{11}\sinh[Z_0(X-L_0)]}{\sigma_{12}\sinh[Z_0(L_S-L_0)]}\\ \dfrac{\sigma_{11}\{Z_1\cosh[Z_1(1-X)]+\psi Z_0^2\sinh[Z_1(1-X)]\}}{\sigma_{12}\{\psi Z_0^2\sinh[Z_1(1-L_S)]+Z_1\cosh[Z_1(1-L_S)]\}}\end{bmatrix}\begin{matrix}\text{for } (0\leqslant X\leqslant L_0)\\ \text{for } (L_0\leqslant X\leqslant L_S)\\ \text{for } (L_S\leqslant X\leqslant 1)\end{matrix} \tag{24}$$

where

$$\sigma_{11}=\cosh[Z_1(1-L_S)]\langle\theta_dZ_0\{\psi Z_0^2\tanh[Z_1(1-L_S)]+Z_1\}-\mu Z_1\sinh[Z_0(L_S-L_0)]\{Z_1\tanh[Z_1(1-L_S)]+\psi Z_0^2\}\rangle \tag{25}$$

and

$$\sigma_{12}=\cosh[Z_0(L_S-L_0)]\{\psi Z_0^3\sinh[Z_1(1-L_S)]+Z_0^{Z_1}\}+\psi Z_0^2(1-\mu^m)\sinh[Z_0(L_S-L_0)]\cosh[Z_1(1-L_S)]\times\{\psi Z_0^2\tanh[Z_1(1-L_S)]+Z_1\} \tag{26}$$

Here it is to mention that to calculate the temperature distribution in a partially wet SRC fin, the linear distance L_0 where the dry and wet parts separated is to be determined on the basis of the continuity of heat conduction at the separating section. It yields the following equations:

$$(1+B\xi)^{1/2}\{\sigma_9+\sigma_{10}(\theta_d+\theta_w)\cosh[Z_3(L_0-L_S)]\}\times\{Z_1+\psi Z_0^2\tanh[Z_1(1-L_0)]\}-\theta_d\sigma_{10}\sinh[Z_3(L_0-L_S)]\times\{\psi Z_0^2+Z_1\tanh[Z_1(1-L_0)]\}=0\quad\text{for } (L_S\leqslant L_0<1) \tag{27}$$

and

$$(1+B\xi)^{1/2}\sinh[Z_0(L_S-L_0)]\{\sigma_{12}(1+\theta_w)-\sigma_{11}(\theta_d+\theta_w)\times\cosh(Z_2L_0)\}+\sinh(Z_2L_0)\{\sigma_{11}+\theta_d\sigma_{12}\cosh[Z_0(L_S-L_0)]\}=0\quad\text{for } 0<L_0\leqslant L_S \tag{28}$$

For a given thermophysical, psychometric and geometric parameters, the root of the above equations L_0can be determined by using Newton–Raphson iterative procedure [26]. A specified convergence for Newton–Raphson method [26] has been taken as 10^{-8} for the final value of L_0.

2.4. Heat transfer rate

The heat transfer rate through the fin is calculated from the temperature distribution in the fin. It can be obtained from the Fourier's law of heat conduction applied to the fin base for fully dry, partially wet and fully wet conditions of a SRC fin, separately, which is in dimensionless form as follows:

Fully dry fin

$$Q_{dry}=\begin{cases}[q_{dry}h^{m-1}m]/[2k^m(T_a-T_b)\pi^{m-1}]\\ \dfrac{\psi Z_0\{\tau_1\sinh[Z_1(1-L_S)]+\tau_2\cosh[Z_1(1-L_S)]\}}{\sigma_3\sinh[Z_1(1-L_S)]+\sigma_4\cosh[Z_1(1-L_S)]}\end{cases} \tag{29}$$

where

$$\begin{bmatrix}\tau_1\\ \tau_2\end{bmatrix}=\begin{bmatrix}\psi Z_0^3\sinh(Z_0L_S)+Z_0^2\{1+(1-\mu^m)Z_0^2\psi^2\}\cosh(Z_0L_S)\\ Z_0Z_1\{\sinh(Z_0L_S)+\psi Z_0\cosh(Z_0L_S)\}\end{bmatrix} \tag{30}$$

Fully wet fin

$$Q_{wet}=\begin{cases}[q_{wet}h^{m-1}m]/[2k^m(T_a-T_b)\pi^{m-1}]\\ \dfrac{Z_2\psi(1+\theta_w)\{\tau_3\sinh[Z_3(1-L_S)]+\tau_4\cosh[Z_3(1-L_S)]\}}{\sigma_7\sinh[Z_3(1-L_S)]+\sigma_8\cosh[Z_3(1-L_S)]}\end{cases} \tag{31}$$

where

$$\begin{bmatrix}\tau_3\\ \tau_4\end{bmatrix}=\begin{bmatrix}\psi Z_2^3\sinh(Z_2L_S)+Z_2^2\{1+\psi^2Z_0^2(1-\mu^m)(1+B\xi)^{1/2}\}\cosh(Z_2L_S)\\ Z_2Z_3\{\sinh(Z_2L_S)+\psi Z_2\cosh(Z_2L_S)\}\end{bmatrix} \tag{32}$$

Partially wet fin

$$[Q_p]=\begin{cases}[q_p h^{m-1}m]/[2k^m(T_a-T_b)\pi^{m-1}] & \\ \psi Z_2\begin{bmatrix}\{\sigma_{10}(1+\theta_w)\cosh(Z_2L_S)+\sigma_9\}/\sigma_{10}\sinh(Z_2L_S)\\ \{(1+\theta_w)\cosh(Z_2L_0)+(\theta_d+\theta_w)\}/\sinh(Z_2L_0)\end{bmatrix} & \begin{matrix}\text{for } (L_S\leqslant L_0<1)\\ \text{for } (0<L_0\leqslant L_S)\end{matrix}\end{cases} \tag{33}$$

2.5. Fin efficiency

Fin efficiency is defined as the ratio of actual heat transfer rate through the fin to the rate of ideal heat transfer rate (q_i). The latter is calculated if the entire fin were maintained at its base temperature. Thus the fin efficiency of dry and wet SRC fins can be expressed from its definition as

$$\begin{bmatrix}\eta_{dry}\\ \eta_{wet}\end{bmatrix}=\begin{bmatrix}Q_{dry}/Q_{i,dry}\\ Q_{wet}/Q_{i,wet}\end{bmatrix}\quad\begin{matrix}\text{for fully dry surface}\\ \text{for fully wet surface}\end{matrix} \tag{34}$$

where

$$\begin{bmatrix}Q_{i,dry}\\ Q_{i,wet}\end{bmatrix}=\begin{bmatrix}q_{i,dry}h^{m-1}m/2k^m\pi^{m-1}(T_a-T_b)\\ q_{i,wet}h^{m-1}m/2k^m\pi^{m-1}(T_a-T_b)\end{bmatrix}$$
$$=\frac{Bi^m}{\psi}\begin{bmatrix}2-m+\psi+2(m-1)\{L_S+\mu(1-L_S)\}\\ (1+\theta_w)(1+B\xi)[2-m+\psi+2(m-1)\{L_S+\mu(1-L_S)\}]\end{bmatrix} \tag{35}$$

The fin efficiency of the partially wet SRC fin can directly be obtained from the ratio of actual heat transfer rate to the ideal heat transfer rate calculated with the assumption of the entire fin surface under a fully wet condition. Alternatively, the efficiency of the partially wet fin can be determined by taking into account of the weighted average of dry and wet surface efficiencies. It can be expressed as

$$\begin{bmatrix}\eta_p\\ \eta_p\end{bmatrix}=\begin{bmatrix}\rho_1\eta_{wet}+\rho_2\eta_{dry}\\ L_0\eta_{wet}+\rho_3\eta_{dry}\end{bmatrix}\quad\begin{matrix}(L_S\leqslant L_0<1)\\ (0<L_0\leqslant L_S)\end{matrix} \tag{36}$$

where

$$\begin{bmatrix}\rho_1\\ \rho_2\\ \rho_3\end{bmatrix}=\frac{1}{L_S+\mu^{m-1}(1-L_S)+\psi/m}\begin{bmatrix}\mu^{m-1}L_0+L_S(1-\mu)(m-1)+\psi(1-\mu^m)/m\\ \mu^{m-1}(1-L_0)+\mu^m\psi/m\\ L_S-L_0+\mu^{m-1}(1-L_S)+\psi/m\end{bmatrix} \tag{37}$$

2.6. Optimization

From the existing literature [19–22], the researchers have concentrated on the optimization of fins for either the dry or the fully wet surface. However, depending upon the thermo-psychometric parameters, the entire fin surface may not participate in condensation process. Thus in this study, an effort has been made to determine analytically the optimum dimensions of longitudinal and pin fins of SRC profile under fully dry, fully wet and partially wet conditions. The volume of both the longitudinal and pin fins with a SRC profile is expressed in non-dimensional form as

$$U=\begin{cases}h^{m+1}vm/[2k^{m+1}\pi^{m-1}]\\ Bi^{m+1}[\mu^m+L_S(1-\mu^m)]/\psi\end{cases} \tag{38}$$

From the expressions of heat transfer and fin volume, it is clear that both these parameters are the functions of Bi, ψ, L_S and μ for a given thermophysical and psychometric parameters. The optimization is done in a generalized form in such a way that either heat transfer or fin volume can be taken as a constraint. Using Lagrange multiplier technique, the optimality criteria is derived which can be expressed as follows:

$$\begin{bmatrix}f_1(Bi,\psi,L_S,\mu)\\ f_2(Bi,\psi,L_S,\mu)\\ f_3(Bi,\psi,L_S,\mu)\end{bmatrix}=\begin{bmatrix}(\partial Q_j/\partial Bi)(\partial U/\partial\psi)-(\partial Q_j/\partial\psi)(\partial U/\partial Bi)\\ (\partial Q_j/\partial\psi)(\partial U/\partial L_S)-(\partial Q_j/\partial L_S)(\partial U/\partial\psi)\\ (\partial Q_j/\partial L_S)(\partial U/\partial\mu)-(\partial Q_j/\partial\mu)(\partial U/\partial L_S)\end{bmatrix}_{j=\text{dry, wet, p}}=\begin{bmatrix}0\\0\\0\end{bmatrix} \tag{39}$$

where the expressions of partial derivative ($\partial U/\partial$Bi), ($\partial U/\partial\psi$), ($\partial U/\partial L_S$), ($\partial U/\partial\mu$), ($\partial Q_j/\partial$Bi), ($\partial Q_j/\partial\psi$), ($\partial Q_j/\partial L_S$) and ($\partial Q_j/\partial\mu$) are derived using Eqs. (29), (31), (33) and (38). In partially wet SRC fins, the amount of heat transfer not only depends on the geometry of the profile but also on the length of the wet part L_0. Therefore, to determine the rate of heat transfer through a partially wet fin, it is essential to evaluate the linear length L_0. Again L_0 is a function of the design and psychometric parameters involved on the optimization process. In order to determine the partial derivative of Q_p with respect to any one of the said variables, the partial derivatives of L_0 with respect to these variables are to be determined. These partial derivatives of L_0 are constructed from Eq. (33) and they can be determined by solving with the help of Newton–Raphson iterative method [26]. Next for solving Eq. (39), one equation for the design constraint is required in the optimization problem. Depending upon the design specification, the constraint equation may be either the fin volume or the heat transfer rate. Thus it can be constructed as given below:

$$[g(Bi,\psi,L_S,\mu)]=\begin{bmatrix}Bi^{m+1}[\mu^m+L_S(1-\mu^m)]/\psi-U\\ [\psi Z_0\{\tau_1\tanh Z_4+\tau_2\}/(\sigma_3\tanh Z_4+\sigma_4)]-Q_{dry}\\ (1+\theta_w)[\psi Z_2\{\tau_3\tanh Z_5+\tau_4\}/(\sigma_7\tanh Z_5+\sigma_8)]-Q_{wet}\\ \psi Z_2[\sigma_{10}(1+\theta_w)\cosh(Z_2L_S)+\sigma_9]/\sigma_{10}\sinh(Z_2L_S)-Q_p\\ \psi Z_2[(1+\theta_w)\cosh(Z_2L_0)+(\theta_d+\theta_w)]/\sinh(Z_2L_0)-Q_p\end{bmatrix}$$
$$=\begin{bmatrix}0\\0\\0\\0\\0\end{bmatrix}\quad\begin{matrix}\\ \\ \\ \text{for } (L_S\leqslant L_0<1)\\ \text{for } (0<L_0\leqslant L_S)\end{matrix} \tag{40}$$

It may be noted that the above equation represents both the constraint equations (fin volume and heat transfer rate). From definition of the fin optimization, any one constraint equation has to be employed during the root finding algorithm. For the solution of Eqs. (39) and (40), Newton–Raphson method can also be applied to obtain the multiple

roots [26]. The basic steps for estimation of multiple roots in the present study are given below:

$$\begin{bmatrix} Bi \\ \psi \\ L_S \\ \mu \end{bmatrix}_{j+1} = \begin{bmatrix} Bi \\ \psi \\ L_S \\ \mu \end{bmatrix}_j + \begin{bmatrix} \Gamma_1/\Gamma \\ \Gamma_2/\Gamma \\ \Gamma_3/\Gamma \\ \Gamma_4/\Gamma \end{bmatrix}_j \tag{41}$$

where the suffixes j and $j+1$ are the j th and $j+1$ th iteration respectively. The expressions for Γ_1, Γ_2, Γ_3, Γ_4 and Γ are given in Appendix. To precede the above iterations, the initial guess values have to be selected in such a way that the convergence criteria will be satisfied in all the steps of iterations. The convergence criterion for the present optimization problem can be adopted as follows [26]:

$$\left\{ \text{Max} \left[\frac{|\partial^2 f_i/\partial Bi^2|}{(\partial f_i/\partial Bi)^2}, \frac{|\partial^2 f_i/\partial \psi^2|}{(\partial f_i/\partial \psi)^2}, \frac{|\partial^2 f_i/\partial L_S^2|}{(\partial f_i/\partial L_S)^2}, \frac{|\partial^2 f_i/\partial \mu^2|}{(\partial f_i/\partial \mu)^2}, \frac{|\partial^2 g/\partial Bi^2|}{(\partial g/\partial Bi)^2}, \frac{|\partial^2 g/\partial \psi^2|}{(\partial g/\partial \psi)^2}, \frac{|\partial^2 g/\partial L_S^2|}{(\partial g/\partial L_S)^2}, \frac{|\partial^2 g/\partial \psi^2|}{(\partial g/\partial \psi)^2} \right] \right\}_{i=1,2,3} < 1 \tag{42}$$

Finally, the optimum parameters like Bi, ψ, L_S and μ are obtained until a specified convergence (10^{-8} in the present study) has been reached.

3. Results and discussion

The moist air consists of two parts; one comprising dry air and other solely of water vapor and they produce a binary mixture. To provide complete definition of its any thermodynamic state, three properties are necessary. One of the three properties can be the composition. The properties of moist air are called the psychometric properties. Ambient pressure, dry bulb temperature and relative humidity are commonly employed to determine a state point of humid air on the psychometric chart. On the basis of the above analysis, results are calculated for a wide range of psychometric properties and a constant ambient pressure.

Before furnishing the result for the present study, it is important to validate the present model via comparison with the published model. It can not be done directly because of the scarcity of results in the existing literature. However, it has already been stated in the earlier section that the analysis of straight fins with the dehumidifying process can be done through the above analysis by taking into consideration of thickness ratio, $\mu = 1.0$. Wu and Bong [7] published an analytical result for the performance analysis of longitudinal fins of straight profile under dehumidifying condition. They have assumed a linear variation of the humidity ratio of the saturated air on the fin surface with its temperature, and an insulated tip condition. Thus the result obtained from the analysis of Wu and Bong [7] can be compared with the result estimated from the analysis of present study for $m = 1$, $\mu = 1$ and $\psi = 0.0$ (for a condition of insulated tip) and this comparison is depicted in Fig. 2. For this, results have been taken for a design parameter selected according to Wu and Bong published paper [7]. From Fig. 2, it is demonstrated that the results predicted by the present and previous models have been matched exactly. Now, some typical results obtained from the present model are illustrated in the following section.

To estimate the temperature distribution in a partially wet fin, the distance L_0 is important. This location separates the wet and dry parts of the fin. In Fig. 3, L_0 of SRC as well as UC profiles for both longitudinal and pin fins is shown as a function of relative humidity RH and a design constant. From Fig. 3, it can be noticed that whether a fin surface becomes a dry, fully wet or partially wet, the air relative humidity is mainly responsible for that. In partially wet fins, L_0 increases at a higher rate with an increase in relative humidity. From this illustration, it can be pointed out that the range of relative humidity for the partially wet surface of a UC profile are 19.67–39.57% and 19.67–56.13% respectively for a longitudinal and a pin fin whereas in case of a SRC profile, this range of relative humidity also depends upon the geometric parameters μ and L_S. It can also be mentioned that for partially wet both longitudinal and pin fins of SRC profile, the range of RH is always higher than that of the UC profile because, for an identical design parameter tip temperature of SRC fins is relatively high. In comparison between the longitudinal and the pin fin with a partially wet SRC profile a smaller range of relative humidity is found in the case of longitudinal fins.

Fig. 4 depicts the variation of temperature on the fin surface (longitudinal and pin fins) of both UC and SRC profiles with the distance from the fin base for the relative humidities of 100% and 70%. The fin parameter Z_0, aspect ratioψ, thickness ratio μ and step length L_S are arbitrarily

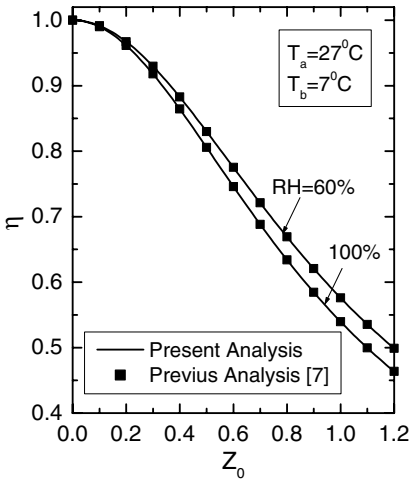

Fig. 2. Comparisons of fin efficiency of a longitudinal rectangular fin in wet conditions evaluated from the present and published models.

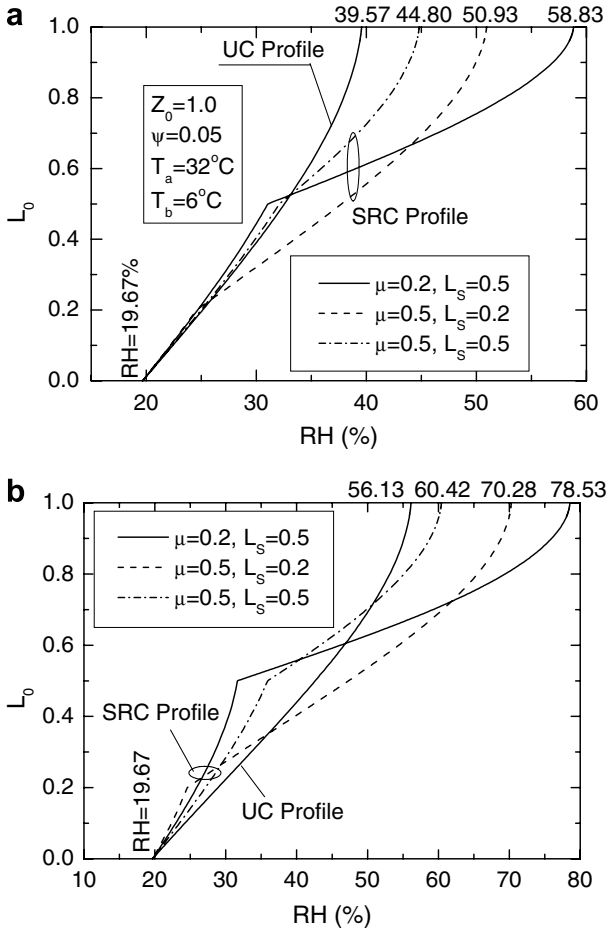

Fig. 3. The linear distance L_0 for partially wet both SRC and UC fins as a function of relative humidity RH: (a) longitudinal fin and (b) pin fin.

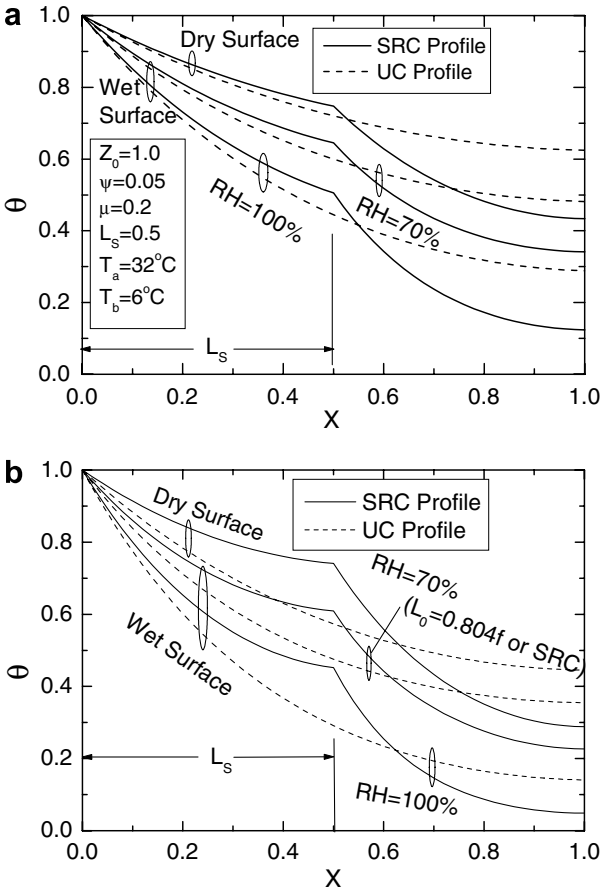

Fig. 4. The variations of temperature distribution in the SRC as well as in the UC fins with the relative humidity of surrounding air: (a) longitudinal fin and (b) pin fin.

chosen as 1.0, 0.05, 0.2 and 0.5, respectively. For these values of design constants, the fin-tip temperature of longitudinal fins of both UC and SRC profiles is below the dew point of the surrounding air as a result, the fin becomes fully wet. In case of pin fins of SRC profile, a partially wet condition is satisfied for the relative humidity of 70%. The temperature distribution on the SRC fin surface for fully dry condition is also depicted in this figure. To facilitate a comparative study, the temperature distribution over the corresponding UC fin is plotted in the same figure. It can be seen from the figure that the temperature distribution in the wet fin is always higher than that in the dry fin because, moisture is condensed on the fin surface by evolving the latent heat of condensation. This may cause to raise a higher fin surface temperature. Again the rate of condensation of water vapor on the fin surface increases with the increase in relative humidity. Therefore, as the relative humidity increases, a gradual rise in temperature in wet surface from that in the dry surface is quite obvious. In comparison with the UC fin, the temperature distribution in the SRC fin shows a peculiar in nature. From the fin base to a distance L_S, the slope of temperature curve in a SRC fin is less steep than in the corresponding UC fin and this slope in a SRC fin changes to a higher value beyond this length. Hence, there is a section in the fin where temperature for both SRC and RC fins is identical. The temperature in a SRC fin beyond this section is always a higher value compared to that in the UC fin.

The fin efficiency of both the longitudinal and pin fins of SRC as well as UC profiles is depicted in Fig. 5 as a function of relative humidity. The variation of relative humidity has been taken over the whole range from 0% to 100%. The fin base temperature is only parameter to fix up a lower limiting value of relative humidity, and below this value, the fin surface is entirely dry. Then there occurs only sensible heat transfer and thus the fin efficiency of dry fins remains constant with the relative humidity for a constant dry bulb temperature. If the relative humidity is above the limiting value, condensation of moisture starts and as a result fin surface becomes a partially wet. The efficiency of partially wet fins decreases with the relative humidity and this change varies sharply for the longitudinal fin of UC profile. In fully wet surface, the overall efficiency of all these fins decreases slightly with the increase in relative humidity. This phenomenon can be interpreted as follows. An increase in the relative humidity causes to an increase in latent heat flux due to more condensation of moisture which affects to increase the local fin surface temperature

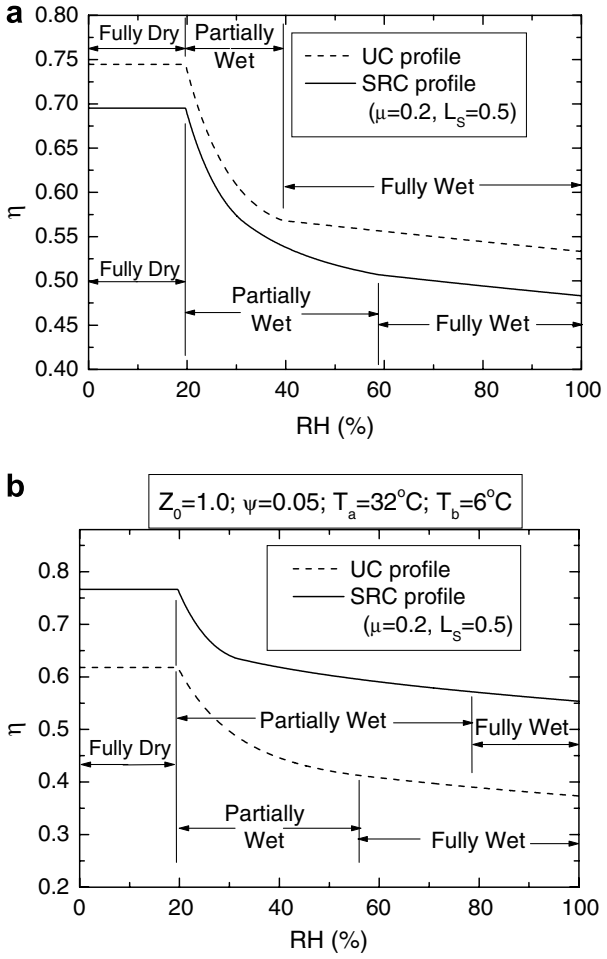

Fig. 5. Fin efficiency of UC and SRC fins as a function of relative humidity RH: (a) longitudinal fin and (b) pin fin.

and consequently to decrease the fin efficiency. For the longitudinal fin, the fin efficiency of SRC profile is always lower than of the UC profile for the identical design parameter. This may be because of a higher variation of temperature in the SRC fin. In case of pin fins, a reversed trend is observed when comparing between UC and SRC profiles. However, for both the longitudinal and pin fins, difference in fin efficiency between an UC and the corresponding SRC profile reduces to a minimum value under the partially wet condition.

The fin efficiency of SRC longitudinal fins under dehumidification of air on the fin surface can be compared vis-à-vis with that of the pin fins with an identical design constant and a psychometric condition which is depicted in Fig. 6. For an identical fin parameter Z_0, thickness ratio μ, aspect ratio ψ, step length parameter L_S, relative humidity RH, dry bulb temperature T_a and base temperature T_b, the overall fin efficiency of a pin fin is always higher than that of the longitudinal fin. This difference in fin efficiency

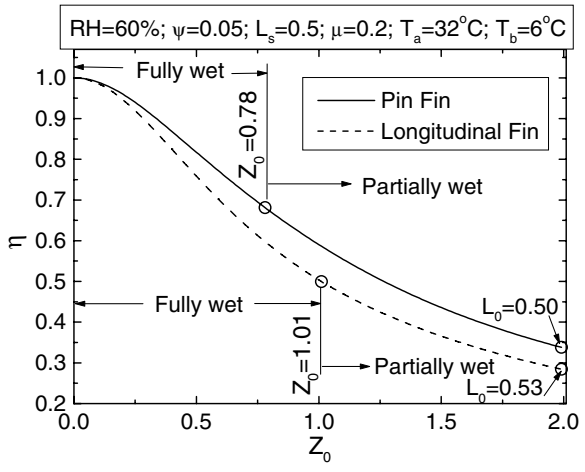

Fig. 6. Fin efficiency of longitudinal and pin fins of SRC profile as a function of fin parameter Z_0.

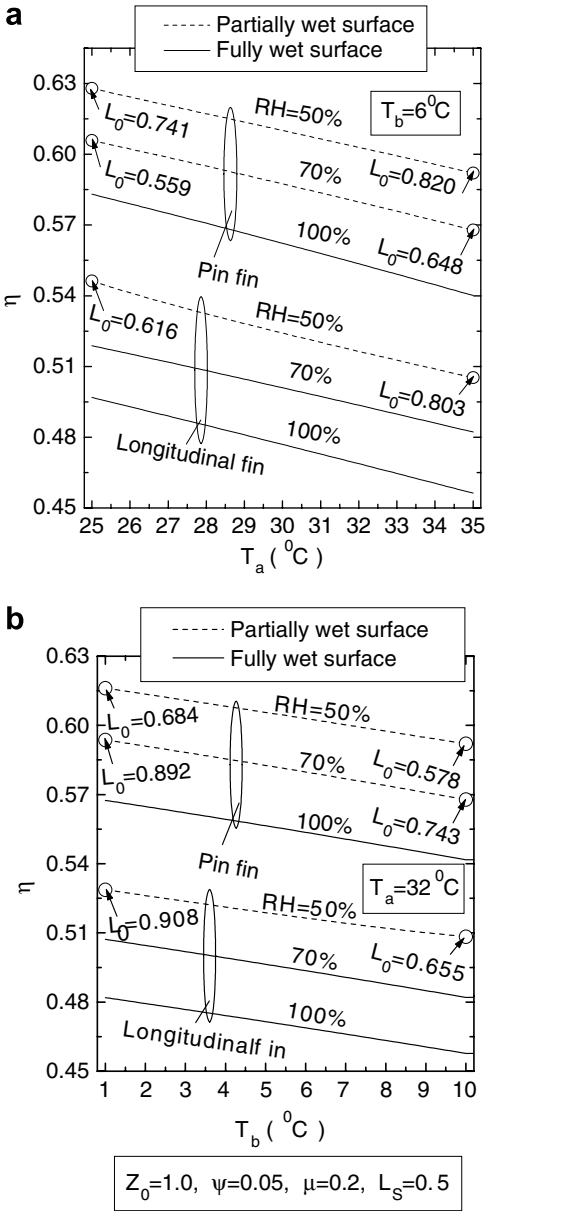

Fig. 7. Variations of fin efficiency of longitudinal and pin fins of SRC profile as a function of (a) dry bulb temperature T_a and (b) fin base temperature T_b.

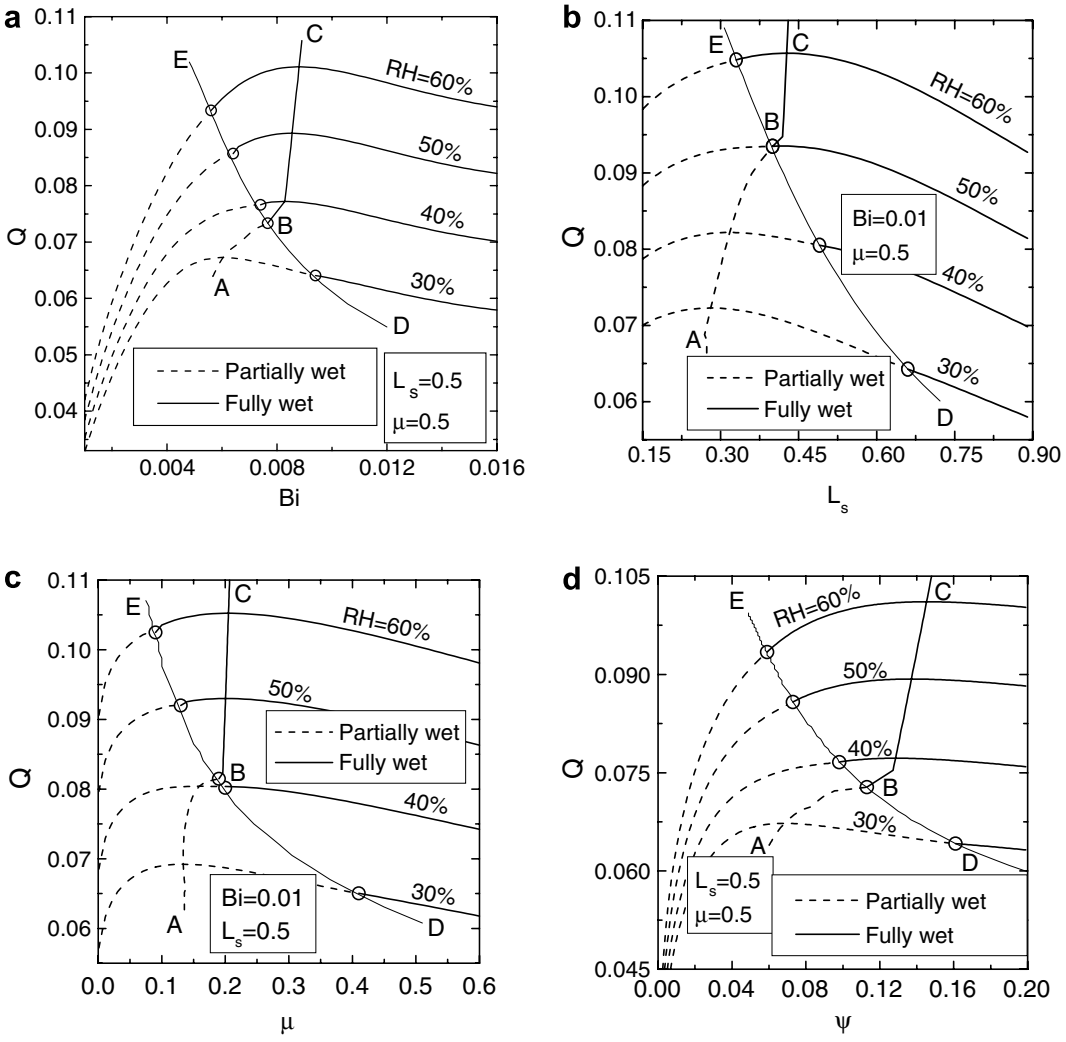

Fig. 8. Heat transfer rate through a SRC longitudinal fin for $T_a = 32$ °C and $T_b = 6$ °C with the variation of (a) *Bi*, (b) L_S, (c) μ, and (d) ψ.

increases initially with Z_0, reaches a maximum value and then declines with the further increase in Z_0. However, this nature is insignificantly varied. It may further be observed from Fig. 6 that, whether the entire or partly fin surface participates in the condensation process, the fin parameter Z_0 is also responsible. The tip temperature gradually increases with the increase in fin parameter Z_0 from its zero value and tip temperature equalizes with the dew point temperature at $Z_0 = 0.78$ and $Z_0 = 1.01$, respectively, for a pin fin and a longitudinal fin. For an increase in Z_0 from the above values, the tip temperature is greater than the dew point and subsequently, fin surface becomes a partially wet. From the same figure, it may also be concluded that a smaller value of fin parameter Z_0 is noticed for the partially wet pin fin in comparison with that for the longitudinal fin under a psychometric condition.

The effect of dry bulb temperature and fin base temperature on the overall fin efficiency of both longitudinal and pin fins with a SRC profile for different constant relative humidities is shown in Fig. 7. For a constant relative humidity, the condensation of moisture on the fin surface increases with the increase in T_a and hence, the fin surface temperature increases. This produces a larger variation in fin temperature in the fin resulting to decrease in fin efficiency as shown in Fig. 7a. A similar observation on the overall fin efficiency is noticed for an increase in fin base temperature T_b with taking a constant ambient temperature T_a as depicted in Fig. 7b. An increase in T_b decreases the wet part of a fin slightly and simultaneously it increases the parameter Z_3 due to increase in B. The first influence is dominated by the second effect and as a result, fin efficiency decreases with T_b.

From Eqs. (39) and (40), it can be mentioned that both the heat transfer rate and fin volume for fully wet SRC fins are functions of the geometrical parameters like *Bi*, ψ, μ and L_S for a given psychometric condition. For a partially wet fin, the rate of heat transfer is also function of L_0. Typical results obtained from the optimization studies are shown in Fig. 8 for constants $T_a = 32$ °C, $T_b = 6$ °C and $U = 0.0005$. The curves are generated in such a way that the heat transfer rate through a longitudinal fin varies with the any one of the said geometrical parameters while the others are taken as a constant. Fig. 8a–d represents the variation of heat transfer as a function of *Bi*, L_S, μ and ψ,

Table 1
Comparisons of an optimum SRC fin with an optimum UC fin for an identical fin volume, relative humidity, ambient temperature ($T_a = 32$ °C) and fin base temperature ($T_b = 6$ °C)

	U	Surface conditions	RH (%)	Rectangular profile				Step profile						Q_r (%)
				L_0	Bi_{opt}	ψ_{opt}	Q_{opt}	L_0	Bi_{opt}	ψ_{opt}	$(L_S)_{opt}$	μ_{opt}	Q_{opt}	
Longitudinal fin	0.00004	Fully dry	–	–	0.00095	0.02257	0.027268	–	0.00139	0.02858	0.4410	0.2643	0.029988	9.98
		Partially wet	40	0.53757	0.00130	0.04255	0.032381	0.43052	0.00189	0.04496	0.3730	0.2098	0.036364	12.30
		Fully wet	60	–	0.00136	0.04659	0.042239	–	0.00272	0.08564	0.2708	0.2658	0.048123	13.93
		Fully wet	80	–	0.00141	0.05008	0.051598	–	0.00308	0.10160	0.2209	0.2681	0.058911	14.17
		Fully wet	100	–	0.00146	0.05324	0.060562	–	0.00337	0.11501	0.1830	0.2719	0.069478	14.72
	0.00008	Fully dry	–	–	0.001519	0.02885	0.034423	–	0.00229	0.03783	0.4230	0.2645	0.037956	10.26
		Partially wet	40	0.60628	0.00210	0.05516	0.040954	0.54782	0.00346	0.06877	0.3153	0.2090	0.046257	12.95
		Fully wet	60	–	0.00220	0.06058	0.053441	–	0.00408	0.10500	0.2286	0.3581	0.060981	14.11
		Fully wet	80	–	0.00229	0.06531	0.065304	–	0.00470	0.12908	0.1470	0.3768	0.074580	14.20
		Fully wet	100	–	0.00236	0.06960	0.076672	–	0.00527	0.14755	0.1396	0.3776	0.087970	14.74
	0.0001	Fully dry	–	–	0.00177	0.03125	0.037110	–	0.00270	0.04162	0.4151	0.2646	0.040963	10.38
		Partially wet	40	0.66432	0.00245	0.06009	0.044180	0.56549	0.00432	0.08183	0.2778	0.2232	0.050046	13.28
		Fully wet	60	–	0.00257	0.05766	0.057610	–	0.00443	0.10313	0.2754	0.3464	0.065827	14.26
		Fully wet	80	–	0.00267	0.07131	0.070469	–	0.00471	0.11421	0.2558	0.3481	0.080803	14.66
		Fully wet	100	–	0.00276	0.07608	0.082747	–	0.00527	0.13519	0.1187	0.3216	0.095932	15.93
	0.0005	Fully dry	–	–	0.00532	0.05659	0.063950	–	0.01257	0.12481	0.1613	0.2787	0.072782	13.81
		Partially wet	40	0.58919	0.00764	0.11674	0.076748	0.51455	0.01287	0.15225	0.2561	0.2996	0.089353	16.42
		Fully wet	60	–	0.00808	0.13070	0.100348	–	0.01390	0.17798	0.2341	0.3053	0.117902	17.49
		Fully wet	80	–	0.00847	0.14349	0.122840	–	0.01479	0.20222	0.1716	0.3505	0.145496	18.44
		Fully wet	100	–	0.00882	0.15567	0.144464	–	0.01444	0.2122	0.1488	0.4226	0.173423	20.05
Pin fin	5.0×10^{-7}	Fully dry	–	–	0.00377	0.10681	0.0002269	–	0.00527	0.1238	0.2226	0.5070	0.000250	9.96
		Fully wet	40	–	0.00472	0.21050	0.0003086	–	0.00611	0.1973	0.2192	0.5215	0.000348	12.83
		Fully wet	60	–	0.00490	0.23487	0.0004108	–	0.00643	0.2168	0.1821	0.5242	0.000467	13.73
		Fully wet	80	–	0.00505	0.25744	0.0005100	–	0.00674	0.2322	0.1398	0.5276	0.000584	14.59
		Fully wet	100	–	0.00519	0.27938	0.0006069	–	0.00698	0.2384	0.0954	0.5308	0.000699	15.09
	1.0×10^{-6}	Fully dry	–	–	0.00501	0.12608	0.0003455	–	0.00680	0.1366	0.2408	0.5064	0.000382	10.62
		Partially wet	40	0.99995	0.00639	0.26054	0.0004725	0.4998	0.00770	0.2386	0.2416	0.5000	0.000540	14.28
		Fully wet	60	–	0.00666	0.29588	0.0006297	–	0.00878	0.2483	0.1757	0.4435	0.000725	15.04
		Fully wet	80	–	0.00692	0.33142	0.0007828	–	0.00938	0.2511	0.1112	0.4035	0.000903	15.35
		Fully wet	100	–	0.00718	0.37142	0.0009329	–	0.01001	0.2628	0.0902	0.3557	0.001080	15.77

respectively. For each of the variation of the above parameters, the rate of heat transfer initially increases, then reaches at maximum value and finally starts declining. The peaks of the curves indicate the optimum design for a specified fin volume and a design constraint. It can be observed that for a given fin volume, the optimum design of a fin is strongly influenced by the relative humidity also. The maximum rate of heat transfer increases substantially for the same fin volume when relative humidity is increased. The curve ABC indicates the loci of maximum heat transfer rate for different relative humidities and a given geometrical parameters. The curve EBD depicts the limiting condition line from which the left hand side represents partially wet surface while the right-side indicates a fully wet surface. From the figure, it can be demonstrated that heat transfer rate is strongly dependent also on the dimensionless geometric parameters Bi, L_S, μ and ψ irrespective of its surface conditions. The dashed and firmed lines represent for partially and fully wet surface conditions respectively. The relative humidity of air plays a key roll to determine whether the optimum point is partially or fully wet. A similar trend is also obtained for pin fins. To avoid repetition for the same nature as shown for longitudinal fins, the result of pin fins with the SRC profile has not been furnished.

Finally, a scheme is established to determine the optimum design parameters of SRC fins in such a way that the rate of heat transfer is maximized for a constraint fin volume. The result of the optimum design parameters is shown in Table 1. It can be mentioned from the table that the Biot number Bi and aspect ratio ψ of an optimum SRC fin increase with the increase of relative humidity and fin volume. From Table 1, it is also highlighted that heat transfer rate through an optimum SRC fin is more than the optimum UC fin for a given fin volume and design condition. However, this difference in heat transfer rate increases with the increase in both relative humidity and fin volume.

4. Conclusions

In this study, an analytical effort has been carried out to determine the performance of both longitudinal and pin fins of SRC profile in fully dry, partially wet and fully wet conditions. The influence of various design and psychometric parameters on the performance of SRC fins has been examined and a comparative study has been made with the UC fin. A generalized optimization scheme of SRC fins has been presented in such way that either maximization of heat transfer rate for a given fin volume or minimization of fin volume for a given heat transfer rate are satisfied. Based on the previous discussion of results, the following conclusions may be summarized as follows:

1. The tip temperature of a SRC fin is always higher than that of the UC fin. However, there is a section in the fin where temperatures of both the longitudinal and pin fins are equal.
2. Depending upon the design parameters and psychometric conditions, fin surface can be treated as fully dry, fully wet or partially wet.
3. The surface temperature of wet fins increases as the relative humidity is increased.
4. The fin performance of wet longitudinal SRC fin is lower than that for the UC fin for a given design condition. For the pin fin, a reversed trend is appeared.
5. The wet fin performance of SRC fins decreases as the dry bulb temperature is increased. A similar observation is also found with the variation of base temperature. However, the effect of dry bulb temperature and base temperature on the wet fin efficiency is exhibited marginally.
6. To maintain a partially wet surface, the range of relative humidity for a SRC fin is always larger than that of the UC fin. However, this range is comparatively more for pin fins.
7. The overall efficiency of wet pin fin is higher than for the longitudinal fin with the same design variables and psychometric conditions.
8. In the case of partially wet fin, the overall efficiency is estimated by the weighted average of dry and wet efficiencies. It can be found that the effect of relative humidity on the fin efficiency for partially wet fin varies significantly.
9. The optimum SRC fin transfers more heat than the optimum UC fin with an identical fin volume. However, this deviation increases with the increase in fin volume and relative humidity.
10. The optimum aspect ratio and Biot number of a SRC fin increase with the increase of relative humidity for an identical fin volume.
11. Whether the fin surface is a dry, fully wet or partially wet at the optimum design, the main deciding factor is air relative humidity. However, the limiting relative humidity for a dry surface is obtained from the fin-base temperature directly. For becoming a partially or fully wet surface, fin volume is responsible slightly.
12. The step length parameter L_S for an optimum SRC fin decreases with the increase in relative humidity and fin volume.

Acknowledgement

The author is indebted to the Jadavpur University funding for the Research Project under Seed Support of Potential for Excellence Scheme (Grant P-1/1057/05) for supporting this study.

Appendix A

$$\Gamma = \begin{vmatrix} \partial f_1/\partial Bi & \partial f_1/\partial \psi & \partial f_1/\partial L_S & \partial f_1/\partial \mu \\ \partial f_2/\partial Bi & \partial f_2/\partial \psi & \partial f_2/\partial L_S & \partial f_2/\partial \mu \\ \partial f_3/\partial Bi & \partial f_3/\partial \psi & \partial f_3/\partial L_S & \partial f_3/\partial \mu \\ \partial g/\partial Bi & \partial g/\partial \psi & \partial g/\partial L_S & \partial g/\partial \mu \end{vmatrix} \quad \text{(A.1)}$$

$$\Gamma_1 = -\begin{vmatrix} f_1 & \partial f_1/\partial\psi & \partial f_1/\partial L_S & \partial f_1/\partial\mu \\ f_2 & \partial f_2/\partial\psi & \partial f_2/\partial L_S & \partial f_2/\partial\mu \\ f_3 & \partial f_3/\partial\psi & \partial f_3/\partial L_S & \partial f_3/\partial\mu \\ g & \partial g/\partial\psi & \partial g/\partial L_S & \partial g/\partial\mu \end{vmatrix} \tag{A.2}$$

$$\Gamma_2 = -\begin{vmatrix} \partial f_1/\partial Bi & f_1 & \partial f_1/\partial L_S & \partial f_1/\partial\mu \\ \partial f_2/\partial Bi & f_2 & \partial f_2/\partial L_S & \partial f_2/\partial\mu \\ \partial f_3/\partial Bi & f_3 & \partial f_3/\partial L_S & \partial f_3/\partial\mu \\ \partial g/\partial Bi & g & \partial g/\partial L_S & \partial g/\partial\mu \end{vmatrix} \tag{A.3}$$

$$\Gamma_3 = -\begin{vmatrix} \partial f_1/\partial Bi & \partial f_1/\partial\psi & f_1 & \partial f_1/\partial\mu \\ \partial f_2/\partial Bi & \partial f_2/\partial\psi & f_2 & \partial f_2/\partial\mu \\ \partial f_3/\partial Bi & \partial f_3/\partial\psi & f_3 & \partial f_3/\partial\mu \\ \partial g/\partial Bi & \partial g/\partial\psi & g & \partial g/\partial\mu \end{vmatrix} \tag{A.4}$$

and

$$\Gamma_4 = -\begin{vmatrix} \partial f_1/\partial Bi & \partial f_1/\partial\psi & \partial f_1/\partial L_S & f_1 \\ \partial f_2/\partial Bi & \partial f_2/\partial\psi & \partial f_2/\partial L_S & f_2 \\ \partial f_3/\partial Bi & \partial f_3/\partial\psi & \partial f_3/\partial L_S & f_3 \\ \partial g/\partial Bi & \partial g/\partial\psi & \partial g/\partial L_S & g \end{vmatrix} \tag{A.5}$$

References

[1] J.I. Threlkeld, Thermal Environmental Engineering, Prentice-Hall, New York, Englewood Cliffs, NJ, 1970.

[2] F.C. McQuiston, Fin efficiency with combined heat and mass transfer, ASRAE J. 81 (1975) 350–355.

[3] A.H. Elmahdy, R.C. Biggs, Efficiency of extended surfaces with simultaneous heat and mass transfer, ASHRAE J. 89 (1983) 135–143.

[4] J.E.R. Coney, H. Kazeminejad, C.G.W. Sheppard, Dehumidification of air on a vertical rectangular fin: a numerical study, Proc. Inst. Mech. Engrs. J. Mech. Eng. Sci. 203 (1989) 165–175.

[5] J.E.R. Coney, C.G.W. Sheppard, E.A.M. El-Shafei, Fin performance with condensation from humid air: a numerical study, Int. J. Heat Fluid Flow 10 (1989) 224–231.

[6] H. Kazeminejad, M.A. Yaghoubi, M. Sepehri, Effect of dehumidification of air on the performance of eccentric circular fins, Proc. Inst. Mech. Engrs. J. Mech. Eng. Sci. 207 (1993) 165–175.

[7] G. Wu, T.Y. Bong, Overall efficiency of a straight fin with combined heat and mass transfer, ASHRAE J. 100 (1994) 367–374.

[8] Y.T. Lin, K.C. Hsu, Y.J. Chang, C.C. Wang, Performance of rectangular fin in wet conditions: visualization and wet fin efficiency, J. Heat Transfer 123 (2001) 827–836.

[9] L.T. Chen, Two-dimensional fin efficiency with combined heat and mass transfer between water-wetted fin surface and moving moist air stream, Int. J. Heat Fluid Flow 12 (1991) 71–76.

[10] S.Y. Liang, T.N. Wong, G.K. Nathan, Comparison of one-dimensional and two-dimensional models for wet surface fin efficiency of a plate-fin-tube heat exchanger, Appl. Therm. Eng. 20 (2000) 941–962.

[11] E. Schmidt, Die Wármeúbertragung dutch Rippen, Zeitschrift des Vereines Deutscher Ingenieure 70 (1926) 885–947.

[12] R.J. Duffin, A variational problem relating to cooling fins, J. Math. Mech. 8 (1959) 47–56.

[13] A.D. Kraus, Sixty-five years extended surface technology, Appl. Mech. Rev. 41 (1988) 321–364.

[14] S. Guceri, C.J. Maday, A least weight circular cooling fin, Trans. ASME J. Eng. Ind. 97 (1975) 1190–1193.

[15] L. Hanin, A. Campo, A new minimum volume straight cooling fin taking into account the length of arc, Int. J. Heat Mass Transfer 46 (2004) 5145–5152.

[16] G. Fabbri, A genetic algorithm for fin profile optimization, Int. J. Heat Mass Transfer 40 (1997) 2165–2172.

[17] D.Q. Kern, A.D. Kraus, Extended Surface Heat Transfer, McGraw Hill, New York, 1972.

[18] A. Aziz, Optimum dimensions of extended surfaces operating in a convective environment, Appl. Mech. Rev. 45 (1992) 155–173.

[19] A. Kilic, K. Onat, The optimum shape for convecting rectangular fins when condensation occurs, Wárme-und Stoffúbertragung 15 (1981) 125–133.

[20] M. Toner, A. Kilic, K. Onat, Comparison of rectangular and triangular fins when condensation occurs, Wárme-und Stoffúbertragung 17 (1983) 65–72.

[21] B. Kundu, An analytical study of the effect of dehumidification of air on the performance and optimization of straight tapered fins, Int. Commun. Heat Mass Transfer 29 (2002) 269–278.

[22] B. Kundu, P.K. Das, Performance and optimization analysis for fins of straight taper with simultaneous heat and mass transfer, J. Heat Transfer 126 (2004) 862–868.

[23] K.G.T. Hollands, B.A. Stedman, Optimization of an absorber plate fin having a step-change in local thickness, Sol. Energy 49 (1992) 493–495.

[24] B. Kundu, P.K. Das, Performance analysis and optimization of annular fin with a step change in thickness, J. Heat Transfer 123 (2001) 601–604.

[25] T.H. Chilton, A.P. Colburn, Mass transfer (absorption) coefficients, Ind. Eng. Chem. 26 (1934) 1183–1187.

[26] J.B. Scarborough, Numerical Mathematical Analysis, Oxford & IBH, New Delhi, 1966.